



# Pharmacokinetics, Mass Balance, and Biotransformation of [<sup>14</sup>C]tinengotinib, A Novel Multi-target Kinase Inhibitor, in Healthy Subjects

Shumao Ni<sup>1</sup> · Sheng Ma<sup>2,3</sup> · Yingying Yu<sup>1</sup> · Zhenwen Yu<sup>4</sup> · Yujia Zhu<sup>1</sup> · Xiaofen Sun<sup>1</sup> · Lin Li<sup>1</sup> · Caixia Sun<sup>1</sup> · Hui Wang<sup>1</sup> · Peng Peng<sup>1</sup> · Zheming Gu<sup>4</sup> · Hua Zhang<sup>2,3</sup> · Frank Wu<sup>1</sup> · Liyan Miao<sup>2,3</sup> · Jean Fan<sup>5</sup>

Accepted: 19 August 2024  
© The Author(s) 2024

## Abstract

**Background and Objective** Tinengotinib, a novel multi-target small molecule kinase inhibitor, is currently undergoing phase II clinical trial in the USA and China. The purpose of this open-label study was to investigate the absorption, metabolism, and excretion of [<sup>14</sup>C]tinengotinib following a single oral dose in healthy subjects.

**Methods** Six healthy male subjects received a single oral dose of [<sup>14</sup>C]tinengotinib capsules at 10 mg/100 μCi, and blood, urine, and feces samples were collected. Phenotyping experiments were further conducted to confirm the enzymes involved in its metabolism.

**Results** Tinengotinib was rapidly absorbed in plasma with a time to peak drug concentration ( $T_{max}$ ) of 1.0–4.0 h post-dose and a long terminal half-life ( $t_{1/2}$ ) of 23.7 h. Blood-to-plasma radioactivity concentration ratios across timepoints ranged from 0.780 to 0.827, which indicated minimal association of radioactivity with blood cells. The mean cumulative excreted radioactivity was 99.57% of the dose, including 92.46% (68.65% as unchanged) in feces and 7.11% (0.28% as unchanged) in urine. In addition to unchanged tinengotinib, a total of 11 radioactive metabolites were identified in plasma, urine, and feces. The most abundant circulating radioactivity was the parent drug in plasma, which comprised 88.23% of the total radioactivity area under the concentration–time curve (AUC). Metabolite M410-3 was a major circulating metabolite, accounting for 5.38% of the parent drug exposure and 4.75% of the total drug-related exposure, respectively. All excreted metabolites accounted for less than 5.10% and 1.82% of the dose in feces and urine, respectively. In addition, no unique metabolites were observed in humans. Tinengotinib was metabolized mainly via CYP3A4.

**Conclusions** Overall, tinengotinib demonstrated a complete mass balance with limited renal excretion, no disproportionate blood metabolism, and slow elimination, primarily through the fecal route. The results of this study provide evidence to support the rational use of tinengotinib as a pharmacotherapeutic agent.

**Registration** ChinadrugTrials.org.cn identifier: CTR20212852.

Shumao Ni and Sheng Ma contributed equally to this work.

✉ Liyan Miao  
miaolysuzhou@163.com

✉ Jean Fan  
fan\_jean@transtherabio.com

<sup>1</sup> Department of Drug Metabolism and Pharmacokinetics, Clinical, Preparation, Chemistry, TransThera Sciences (Nanjing), Inc., Nanjing, China

<sup>2</sup> Department of Pharmacology, the First Affiliated Hospital of Soochow University, Suzhou, China

<sup>3</sup> Institute for Interdisciplinary Drug Research and Translational Sciences, College of Pharmaceutical Sciences, Soochow University, Suzhou, China

<sup>4</sup> Value Pharmaceutical Services Co. Ltd., Nanjing, China

<sup>5</sup> TransThera Sciences (US), Inc., Gaithersburg, MD, USA

## 1 Introduction

Tinengotinib is a first-in-class, spectrum-selective multi-target oral small molecule kinase inhibitor that inhibits fibroblast growth factor receptors (FGFR), vascular endothelial growth factor receptors (VEGFRs), Janus kinases (JAKs), Aurora A/B, and colony stimulating factor 1 receptor (CSF1R) [1]. In a phase I study in patients (NCT03654547), preliminary efficacy indicated potential clinical benefit in patients with cholangiocarcinoma (CCA), triple-negative breast cancer (TNBC), and metastatic castrate-resistant prostate cancer (mCRPC) [2, 3], which are all considered to have urgent unmet clinical need with a poor prognosis and short overall survival [4–6]. Currently, tinengotinib is undergoing phase Ib/II clinical trials in the USA (NCT04742959 and

## Key Points

Tinengotinib demonstrated a complete mass balance, and excretion was predominantly through feces (92.46% in feces and 7.11% in urine).

Tinengotinib is metabolized via CYP3A4, with the parent drug representing 88.23% of total circulating radioactivity AUC and three minor metabolites (each < 5%).

These findings provide support for the clinical pharmacology development program including drug–drug interaction (DDI) potential and special populations investigations.

NCT04919642) and China (NCT05253053) for the treatment of solid tumors including CCA, mCRPC, and HR+/HER2– breast cancer and TNBC.

Therefore, we need to characterize the absorption, metabolism, and excretion (AME) properties of tinengotinib in human body to support the initiation and rational design of late phase development programs, such as potential drug–drug interaction (DDI) and renal or hepatic impairment studies. The present study also helps to identify and quantify differences in drug metabolism between animals conducted in preclinical safety assessments and humans. A better understanding of the metabolic mechanisms and clearance pathways of compounds *in vivo* is vitally important for interpreting pharmacology, pharmacokinetic, and toxicology data.

In current clinical development, tinengotinib 10 mg once a day (QD) has been selected as the recommended phase II dose (RP2D) [7]. Results from the already completed study (NCT04705922), a clinical trial evaluating food effects and the relative bioavailability of tinengotinib in adult healthy volunteers at a dose of 10 mg, indicated that tinengotinib was well tolerated. A single oral dose of 100  $\mu$ Ci was selected for evaluation in the current study, on the basis of preclinical data from tissue distribution and excretion studies [8]. Herein, we investigated the absorption, metabolism, and excretion of [ $^{14}$ C]tinengotinib

following a single peroral dose of two capsules containing approximately 10 mg/100  $\mu$ Ci [ $^{14}$ C]tinengotinib in six healthy male subjects. By combining the results from the previous phenotyping experiments [8], a reaction phenotyping study was also performed with [ $^{14}$ C]tinengotinib to confirm whether the metabolites observed in plasma could be monitored in an *in vitro* system.

## 2 Methods

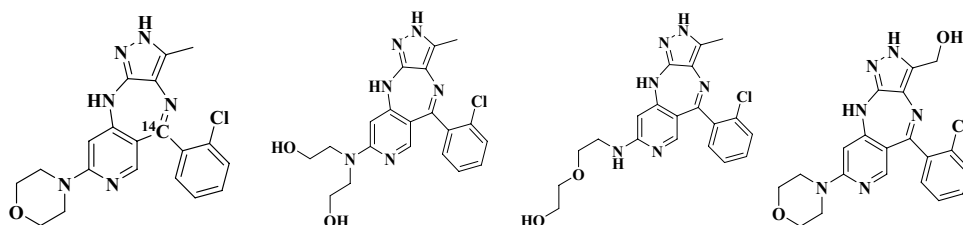
### 2.1 Study Drug and Chemicals

[ $^{14}$ C]Tinengotinib (specific activity 53.1 mCi/mmol, radiochemical purity 99.6%) was provided by Pharmaron UK Ltd. (Northamptonshire, UK). [ $^{14}$ C]Tinengotinib capsules with 5 mg capsule strength (45.3  $\mu$ Ci or 1.677 MBq per capsule) were also provided by Pharmaron UK Ltd. Tinengotinib (assay: 98.7%) for quantitative analysis, *d*<sub>8</sub>-tinengotinib (assay: 92.1%) as internal standard, and the reference substances M412-1 (TT-00925), M412-2 (TT-00890), and M410-3 (TT-02236) for structure confirmation were synthesized in house. The chemical structures of tinengotinib with the position of the radiolabel and its metabolites are shown in Fig. 1.

### 2.2 Study Design and Subjects

This was a phase I, single-center, open-label, nonrandomized single-dose study conducted in six healthy, fasting Chinese male subjects after a single oral dose of 10 mg/100  $\mu$ Ci [ $^{14}$ C]tinengotinib capsules (ChinadrugTrials.org.cn ID: CTR20212852). The primary objectives were to evaluate the pharmacokinetics, mass balance, and biotransformation of tinengotinib in humans. The clinical trial part of the study was conducted at the First Affiliated Hospital of Soochow University (Suzhou, China) as a Clinical Research Unit (CRU). The study was conducted in compliance with the Helsinki Declaration and the International Council for Harmonization Good Clinical Practice guidelines and approved by the hospital ethics board (ethics approval number:

**Fig. 1** Structure of [ $^{14}$ C]tinengotinib with the position of the  $^{14}$ C-label and three reference metabolites



2021230, 12 October 2021). All subjects provided written informed consent prior to study initiation.

Subjects were screened for eligibility within the 7 days before scheduled drug administration and then admitted to the CRU on Day – 2 (the day prior to administration), followed by baseline measurement and sample collection on Day – 1. Six healthy male Chinese subjects aged 18–45 years with a body mass index between 19 and 26 kg/m<sup>2</sup> were enrolled in the study. All enrolled subjects fulfilled the inclusion criteria and did not present with any exclusion criteria. Each of six subjects orally took two [<sup>14</sup>C]tinengotinib capsules after at least 10 h of fasting and approximately 240 mL of warm water. The subjects continued to abstain from food and water for an additional 4 h and 1 h, respectively. Blood, urine, and feces samples were collected up to 288 h after oral administration. A two-stage detection approach was applied to determine whether the sample collection met the following criteria: (1) the cumulative radioactivity excreted in urine and feces exceeds 80% of the administered dose, (2) the radioactivity in urine and feces was less than 1% of the administered dose over a 24 h period on 2 consecutive sample collection days, and (3) the radioactivity concentration for 2 consecutive days in plasma was less than three times the measured value of background.

### 2.3 Sample Collection, Handling, and Storage

Blood, urine, and feces samples were collected at specified times to evaluate the pharmacokinetics (PK), blood/plasma distribution, mass balance, metabolite profiling, and metabolites identification of [<sup>14</sup>C]tinengotinib. The timing of sample collection and storage is described in Supplementary materials section 1.

### 2.4 Safety Assessment

The assessment of safety included adverse events, clinical laboratory tests (routine blood, blood biochemistry, coagulation function, routine urine, and fecal routine with occult blood), ophthalmic examinations, vital signs, 12-lead electrocardiograms (ECGs), and physical examinations. All adverse events were performed according to the Common Terminology Criteria for Adverse Events (CTCAE) version 5.0.

### 2.5 Determination of Total Radioactivity

The total radioactivity in blood, plasma, urine, and feces was determined by the liquid scintillation counter (LSC; Tri-Carb 4910<sup>TR</sup>) using Ultima Gold<sup>TM</sup> cocktail (Perkin Elmer, MA, USA) as the liquid scintillation cocktail. Quenching correction using the external standard method was used for

the determination of liquid scintillation counter biological sample. The LSC was programmed to automatically subtract instrument background (blank sample) and to convert counts per minute (CPM) to disintegrations per minute (DPM). Duplicate aliquot of plasma and urine was weighed and then mixed scintillation cocktail and counted directly. Each fecal sample was mixed with an appropriate volume of isopropanol/water (50/50, v/v) and then homogenized after overnight immersion in the refrigerator at 1–9 °C. Duplicate aliquots of blood and fecal homogenates were weighed and combusted by a biological oxidizer (HTC-501; Hualida Experimental Equipment, Suzhou, China) prior to LSC.

### 2.6 Determination of Tinengotinib in Plasma

The concentration of tinengotinib in human plasma was determined after protein precipitation using a validated liquid chromatography tandem mass spectrometry (LC-MS/MS) method. Briefly, aliquots of 100 µL plasma were mixed with 20 µL internal standard (IS, 250 ng/mL) and extracted by adding 500 µL acetonitrile. After vortex mixing, the samples were centrifuged at 3200×g and 4 °C for 5 min. Subsequently, 400 µL of the supernatant was transferred to another clean 96-well collection plate and evaporated to dryness under a nitrogen stream. The dried residues were reconstituted with 200 µL of 10 mM ammonium acetate in water/acetonitrile (65:35, v:v), which were the initial proportion of mobile phase A and B, respectively. Subsequently, 5 µL of reconstituted sample was then subjected to LC-MS/MS analysis. Tinengotinib and IS were separated using an ACE Excel 3 C18-AR, 50 × 2.1 mm, 3 µm column (ACT, UK) at a flow rate of 0.4 mL/min. The LC-MS/MS system consisted of a Shimadzu HPLC 30-AD (Kyoto, Japan) interfaced to an API 5500 mass spectrometer (AB Sciex, Singapore) with positive electrospray ionization (ESI) mode with multiple reaction monitoring (MRM) detection. The quantitative ion transition for tinengotinib is from *m/z* 395.1 to *m/z* 351.1 and *m/z* 403.1 to *m/z* 355.1 for internal standard.

### 2.7 Pharmacokinetic Analysis

Pharmacokinetic (PK) parameters of total radioactivity and tinengotinib concentration in plasma were performed using non-compartmental methods in the validated software program Phoenix WinNonlin 8.3 (Certara, Princeton, NJ, USA), which was used to generate descriptive statistics and plot concentration–time curves. The following PK parameters were evaluated: maximum observed concentration ( $C_{\max}$ ), time to reach  $C_{\max}$  ( $T_{\max}$ ), area under the concentration–time curve (AUC) from time zero to last quantifiable concentration ( $AUC_{0-t}$ ), AUC from time zero extrapolated to infinity ( $AUC_{0-\infty}$ ), terminal half-life ( $t_{1/2}$ ), mean residence time

(MRT), clearance ( $CL/F$ ), and apparent volume of distribution during the terminal phase ( $V_z/F$ ). The total radioactivity ratio of whole blood-to-plasma at each time point was calculated as a ratio of concentrations in blood to concentrations in plasma.

## 2.8 Sample Preparation for Metabolic Radio-Profiling

The extracted and reconstituted samples from plasma, urine, and fecal homogenate were radio-assayed before and after extraction. The plasma and urine pellets were dissolved in 1 N KOH solution before LSC, and fecal homogenates and the post extracted residues were combusted by a biological oxidizer before LSC. The resultant data was used to determine the extraction efficiency and the method recovery of radioactivity.

### 2.8.1 Plasma

Plasma from each of the six subjects at 0–96 h or 0–120 h post-dose, which covered > 90% of the total radioactivity exposure, was pooled across subjects according to the Hamilton pooling method [9] to obtain six AUC-pooling samples of  $AUC_{0-96h}/AUC_{0-120h}$  and one single-plasma AUC pooled sample of all subjects. Equal-volume aliquots of plasma samples from 0.5 h, 2 h, 8 h, and 24 h were pooled across the time points to obtain four time-point-pooled plasma samples. Pooled plasma samples were extracted by protein precipitation using threefold volumes of acetonitrile containing 0.1% formic acid. After vortex mixing, the mixture was sonicated for 5 min and stored in a refrigerator at 4 °C for 30 min, followed by centrifuging at 10000  $\times g$  and 4 °C for 10 min. The supernatant was separated and the post-extraction solids (PES) were suspended with onefold volume of water and thereafter extracted with twofold volumes of methanol containing 0.1% formic acid. The above operation was repeated twice, and the three extracts were combined and evaporated to dryness under a stream of nitrogen at room temperature. The residues were reconstituted in acetonitrile/water (50:50, v:v) and injected into high-performance liquid chromatography (HPLC) radio-profiling.

### 2.8.2 Urine

Urine from each of the six subjects at 0–72 h post-dose, representing > 85% of the total radioactive in urinary excretion, was pooled across subjects by equal percentage of volume to obtain six 0–72 h urine samples. Equal-volume aliquots of urine samples from 0 to 12 h, 12 to 24 h, and 24 to 72 h were pooled across time intervals to obtain three time-interval-pooled urine samples. The pooled urine samples were extracted by adding fivefold volumes

of acetonitrile containing 0.1% formic acid, vortexed for 5 min and sonicated for 5 min. Then, the mixture was centrifuged at 10000  $\times g$  and 4 °C for 10 min. The supernatant was separated from the PES and evaporated to dryness under a nitrogen stream at room temperature. The residues were reconstituted in acetonitrile/water (1:9, v:v) and injected into HPLC radio-profiling.

### 2.8.3 Fecal

Fecal homogenate from each of the six subjects at 0–192 h post-dose was pooled across subjects by equal weight percentages to obtain six 0–192 h fecal samples that represented approximately 90% of the total radioactive in fecal excretion. Fecal homogenate was pooled from 0 to 24 h, 24 to 72 h, and 72 to 192 h at equal percent weight across time intervals to obtain three time-interval-pooled fecal samples. The pooled fecal samples were extracted with fivefold volumes of acetonitrile containing 0.1% formic acid. After extraction, the samples were vortexed for 5 min and sonicated for 5 min, followed by centrifuging at 10000  $\times g$  and 4 °C for 10 min. The supernatant was transferred to another clean tube, and then the PES was re-extracted twice with 1 mL water and twofold volume of acetonitrile containing 0.1% formic acid. The combined extracts were evaporated to dryness under a stream of nitrogen at room temperature. The residues were reconstituted with acetonitrile/water (50:50, v:v) and injected into HPLC radio-profiling.

## 2.9 Metabolite Radio-Profiling and Identification

The reference standard of [ $^{14}C$ ]tinengotinib was directly subjected to a Shimadzu CBM-20A HPLC system coupled with an online radiochemical monitor (RAM; v-ARC<sup>TM</sup> Radio-LC System, model 3; Aim Research Company, USA), and HPLC radio-chromatograms were processed by using ARC Data system 3 (Version: 3.0.2.379). Tinengotinib and its metabolites in plasma, urine, and feces were performed using a HPLC system with off-line radioactivity detection using a Waters Xselect HSS T3 column (4.6  $\times$  250 mm, 3.5  $\mu m$ , maintained at 40 °C) and a column filter of the same type. The mobile phase consisted of 0.4% formic acid in water adjusted to pH3.2 with ammonium hydroxide (solvent A) and acetonitrile (solvent B). The co-effluent metabolites (M420-3 and M570-1) were further subjected to a secondary separation using an ACE Excel 3 C18, 150  $\times$  4.6 mm column (maintained at 40 °C) with gradient analysis (mobile phase A: 20 mM ammonium acetate solution adjusted to pH 5.50 with acetic acid, mobile phase B: methanol). HPLC effluent was collected at 15 s intervals by automatic fraction collector (Foxy<sup>®</sup>R2; Teledyne Isco, Nebraska, USA) and fractionated into Deep-well LumaPlate<sup>TM</sup>-96 plates (Perkin Elmer). The plates were subsequently dried by a Savant

SpeedVac® concentrator (SC250DDA-120; Thermo Fisher Scientific, San Jose, CA), followed by solid scintillation counting using a MicroBeta<sup>2</sup> plate counter (2450-0120, Perkin Elmer). HPLC radio-chromatograms were reconstructed using ARC® Convert and Evaluation software to obtain the off-line radio-profiling.

Metabolites in pooled plasma, urine, and feces samples were characterized or identified utilizing liquid chromatography-radiochemical activity monitor-mass spectrometry (LC-RAM/MS), run on a Q Exactive mass spectrometer (Thermo Scientific) equipped with a turbo ion spray (electrospray) interface in a positive ion mode. Higher-energy collisional dissociation (HCD) fragmentation on mass-selected of the protonated molecular ion was performed in parallel with full-scan high resolution Fourier-transform mass spectrometry (FTMS). Structures of metabolites were proposed by comparing the exact mass, the mass spectral fragmentation patterns, metabolic pathways, and HPLC retention time with the parent tinengotinib under the same experimental conditions. The structures of metabolites were also confirmed by comparison with synthetic reference substances.

## 2.10 Phenotyping Assay

Results of the previous CYP phenotyping studies of unlabeled tinengotinib [8] showed that CYP3A4, CYP2C8, and CYP2D6 were involved in the metabolism of tinengotinib. Furthermore, a reaction phenotyping experiment in current study was conducted using [<sup>14</sup>C]tinengotinib incubate in human recombinant CYP450 (rCYP) enzymes CYP2C8, CYP2D6, and CYP3A4 and non-CYP450 enzymes FMO3, AO, and XO; human liver S9 (HL-S9); and human liver microsomes (HLM) in 100 mM phosphate buffer (pH = 7.4). The final incubation system consisted of 50 pmol/mL human recombinant CYP450 enzymes, 40 pmol/mL recombinant human non-CYP450 enzymes, 0.5 mg/mL HL-S9 or 0.5 mg/mL HLM, 5 mM MgCl<sub>2</sub>, 1 mM or 2 mM nicotinamide adenine dinucleotide phosphate reduced (NADPH, Saint Louis, USA), and 10 μM [<sup>14</sup>C]tinengotinib (specific activity: 26.55 mCi/mmol). A negative control was conducted under the same conditions in the absence of recombinant human CYP450 enzymes and non-P450 enzymes, HLM, or HL-S9. The incubation system was initiated by the addition of NADPH after 5 min pre-incubation in a 37 °C water bath. After 60 min or 120 min incubation, cold acetonitrile was added to terminate the reaction and vortexed for 3 min, followed by centrifugation at 10000 ×g and 4 °C for 10 min. The supernatant was transferred to a clean 15 mL tube, and then the PES was re-extracted twice with water and acetonitrile. The combined extracts were evaporated under a stream of nitrogen at room temperature. The residues were reconstituted with methanol/water (50:50, v:v) and centrifuged at 10000 ×g and 4 °C for 10 min. The supernatants were

analyzed by LC-RAM/MS for radio-profiling and metabolite structural identification.

## 3 Results

### 3.1 Safety Assessment

A total of six healthy Chinese adult male subjects completed the study. None of the subjects experienced vomiting throughout the study period, and there were no previous/concomitant medications that affected the pharmacokinetics of tinengotinib. One of six subjects experienced one adverse event 13 days after administration. This one adverse event was an increase in alanine aminotransferase (ALT). This adverse event was defined as grade 1 according to the Medical Dictionary for Regulatory Activities (MedDRA, Chinese version 25.0). After 5 days, the subject recovered completely without the need for therapeutic intervention. No other adverse events were reported. There were no clinically significant findings in any laboratory evaluations, ophthalmic examinations, vital sign assessments, ECGs, and physical examinations. Therefore, the results in this study suggest tinengotinib was generally well tolerated and safe.

### 3.2 Pharmacokinetics of Total Radioactivity and Tinengotinib

Mean concentration versus time curves of total radioactivity (TRA) in plasma or blood, and tinengotinib (parent) in plasma are presented in Fig. 2, and main pharmacokinetic parameter for the TRA and tinengotinib in plasma are summarized in Table 1. Following a single oral dose of [<sup>14</sup>C]tinengotinib capsules at 10 mg/100 μCi in six healthy, fasting male adult subjects, the median  $T_{max}$  of TRA and tinengotinib in plasma were all reached after approximately 2.00 h. Thereafter, the concentration of TRA and tinengotinib declined with the mean  $t_{1/2}$  values of 23.7 h and 35.5 h, respectively. For the exposure of tinengotinib and TRA in plasma, the mean  $C_{max}$  values were 63.3 ng/mL and 84.9 ng Eq/mL, and the mean  $AUC_{0-\infty}$  values were 1640 h·ng/mL and 2480 h·ng Eq/mL, respectively. The mean  $CL/F$  and  $V_z/F$  for tinengotinib were 6.20 L/h and 210 L, respectively, compared with 4.08 L/h and 206 L for the TRA, respectively. In addition, the mean blood-to-plasma radioactivity concentration ratios across timepoints ranged from 0.780 to 0.827 after administration.

### 3.3 Excretion and Mass Balance of Radioactivity in Urine and Feces

The mean cumulative excretion of radioactivity in urine and feces over 288 h is illustrated in Fig. 3. After oral

**Fig. 2** Total radioactivity in blood or plasma and tinengotinib (parent) in plasma versus time curves after a single oral dose of [ $^{14}\text{C}$ ]tinengotinib capsules (mean  $\pm$  standard deviation,  $N = 6$ )

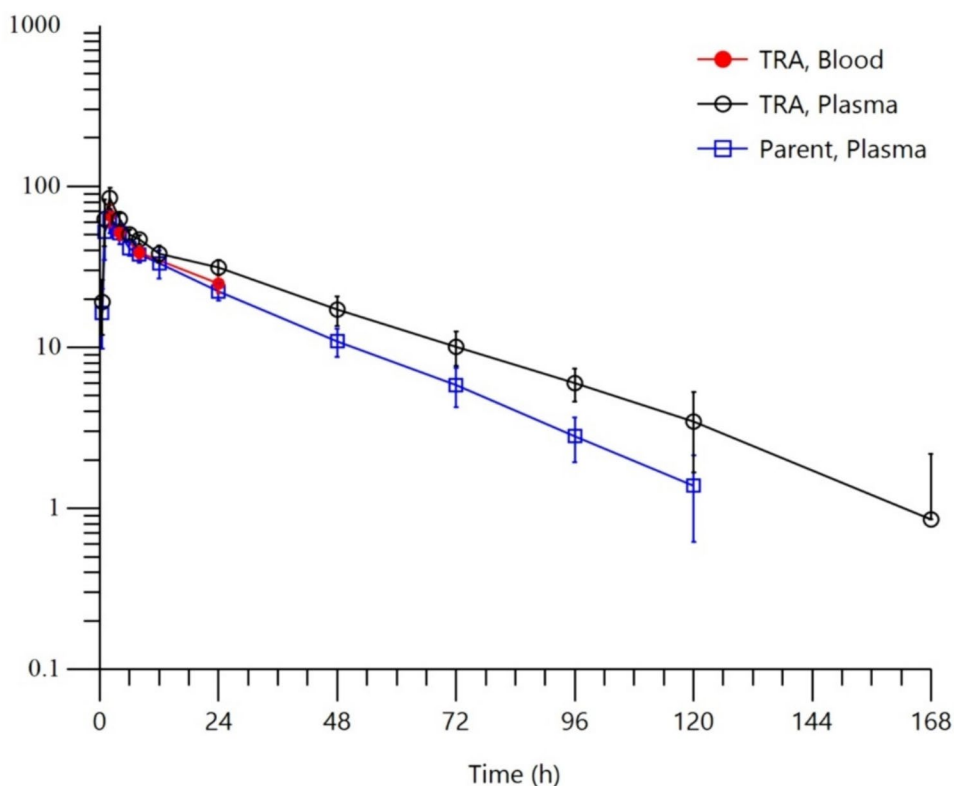


**Table 1** Pharmacokinetic parameters of total radioactivity and tinengotinib in human plasma after a single oral dose of [ $^{14}\text{C}$ ]tinengotinib capsules (Mean  $\pm$  SD,  $N = 6$ )

Parameter	Unit	Total radioactivity	Tinengotinib
$T_{\max}^a$	h	2.00 (2.00, 2.02)	2.00 (1.00, 4.00)
$C_{\max}$	ng Eq/mL <sup>b</sup>	84.9 $\pm$ 12.7	63.3 $\pm$ 7.52
$\text{AUC}_{0-t}$	h-ng Eq/mL <sup>b</sup>	2310 $\pm$ 284	1590 $\pm$ 219
$\text{AUC}_{0-\infty}$	h-ng Eq/mL <sup>b</sup>	2480 $\pm$ 293	1640 $\pm$ 232
$\text{MRT}_{0-t}$	H	35.4 $\pm$ 6.99	28.5 $\pm$ 3.41
$t_{1/2}$	H	35.5 $\pm$ 8.32	23.7 $\pm$ 2.80
$V_z/F$	L	206 $\pm$ 38.6	210 $\pm$ 27.6
$\text{CL}/F$	L/h	4.08 $\pm$ 0.518	6.20 $\pm$ 0.958

SD standard deviation

<sup>a</sup>The median (minimum and maximum) value are provided in the table

<sup>b</sup>The unit of  $C_{\max}$  and AUC for tinengotinib is ng/mL and h-ng/mL, respectively

administration, TRA was excreted similarly in six healthy male adult subjects with little inter-individual variation. The overall mean recovery of radioactivity in urine and feces samples was  $99.57\% \pm 0.77\%$  (98.68–108.81%). The majority of the radioactivity was recovered in the first 120 h post-dose (5 days), accounting for 92.95% of the administered dose and 93.35% of the total recovery, respectively. After

168 h post-dose, the daily excretion was less than 1% of the dose. The major route of excretion of radioactivity was via the feces, accounting for  $92.46\% \pm 0.94\%$  of the dose, whereas only  $7.11\% \pm 0.82\%$  was recovered in the urine.

### 3.4 Metabolite Profiling and Identification in Plasma, Urine, and Feces

Mean radioactivity distribution of [ $^{14}\text{C}$ ]tinengotinib and its metabolites in plasma, urine and feces are shown in Table 2. Representative HPLC radio-chromatogram is presented in Fig. 4. In addition to unchanged tinengotinib, a total of 11 radioactive metabolites in plasma, urine, and feces were tentatively identified by LC-MS/MS, including mono-oxidation (M410-1 and M410-3), di-oxidation (M426-2), glucuronidation of M426-2 (M602), oxidative cleavage of morpholine ring (M412-1 and M412-2), glucuronidation of M412-1 and M412-2 (M588-1 and M588-2), oxidation and de-ethylation of the morpholine ring to carboxylic acid (M382), glucuronidation (M570-1), and cystein conjugation (M513), as shown in Fig. 5. The structures of M410-3, M412-1, and M412-2 were confirmed by the synthetic reference substances. The structures of the metabolites were primarily determined on the basis of retention times and the mass difference between the protonated molecular ion and the calculated molecular ion. This was done in comparison with the key ion

**Fig. 3** Mean cumulative excretion of radioactivity within 288 h after a single oral dose of [<sup>14</sup>C]tinengotinib capsules (mean ± standard deviation, *N* = 6)

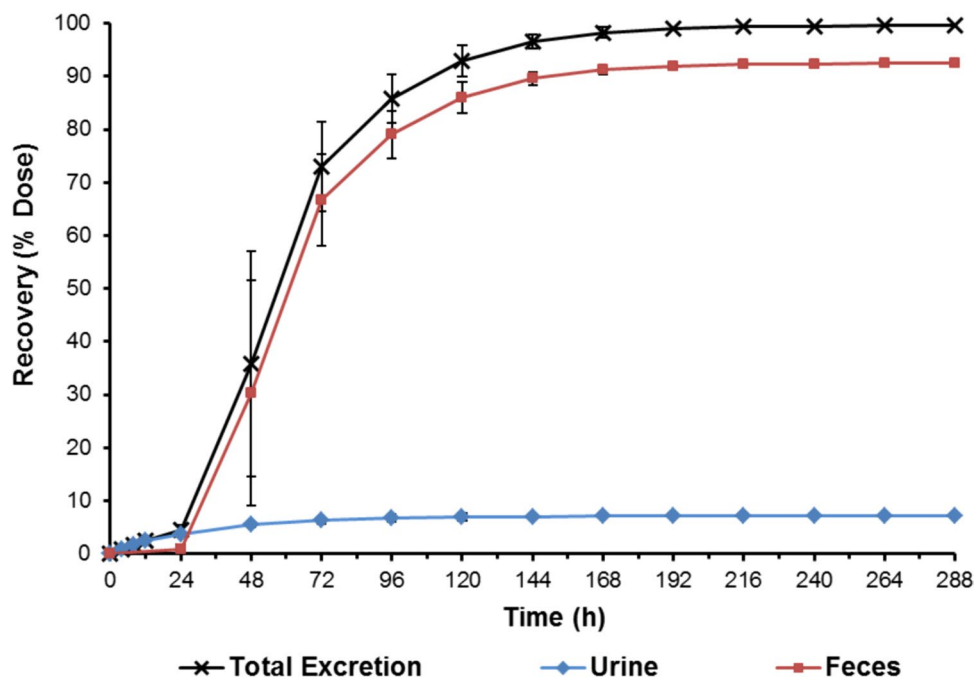


**Table 2** Mean radioactivity distribution of [<sup>14</sup>C]tinengotinib and its metabolites in plasma, urine, and feces

Metabolites	Modification	Plasma		Urine	Feces	Feces + urine
		%AUC	M/P (%) <sup>a</sup>	%Dose	%Dose	%Dose
Tinengotinib	Parent compound	88.23	NA	0.28	68.65	68.93
M602	Glucuronidation of M426-2	ND	NA	0.19	ND	0.19
M588-1	Glucuronidation of M412-1 (TT-00925)	ND	NA	0.24	ND	0.24
M588-2	Glucuronidation of M412-2 (TT-00890)	ND	NA	0.65	ND	0.65
M410-1	Mono-oxidation	ND	NA	0.43	1.76	2.19
M382	Oxidation and de-ethylation of morpholine ring to carboxylic acid	ND	NA	0.37	1.23	1.60
M412-1 (TT-00925)	Oxidative cleavage of morpholine ring	0.06	0.07	0.19	2.72	2.91
M426-2	Di-oxidation	ND	NA	0.38	5.10	5.48
M412-2 (TT-00890)	Oxidative cleavage of morpholine ring	0.06	0.07	0.31	3.14	3.45
M410-3 (TT-02236)	Mono-oxidation	4.75	5.38	0.46	3.00	3.46
M570-1	Glucuronide conjugation	2.54	2.88	1.82	1.60	3.42
M513	Cysteine conjugation	ND	NA	ND	0.84	0.84
Total of identified radioactivity <sup>b</sup>		95.64		5.32	88.04	93.36
Total of unidentified radioactivity <sup>c</sup>		3.09		1.82	4.45	6.27
Percentage of identified radioactivity <sup>d</sup>		95.64		74.82	95.22	93.76

ND not detected, NA not applicable

<sup>a</sup>Ratio of metabolites to parent compound in plasma

<sup>b</sup>Ratio of peak area of identified radioactive peak to total plasma radioactive exposure or to dose administered

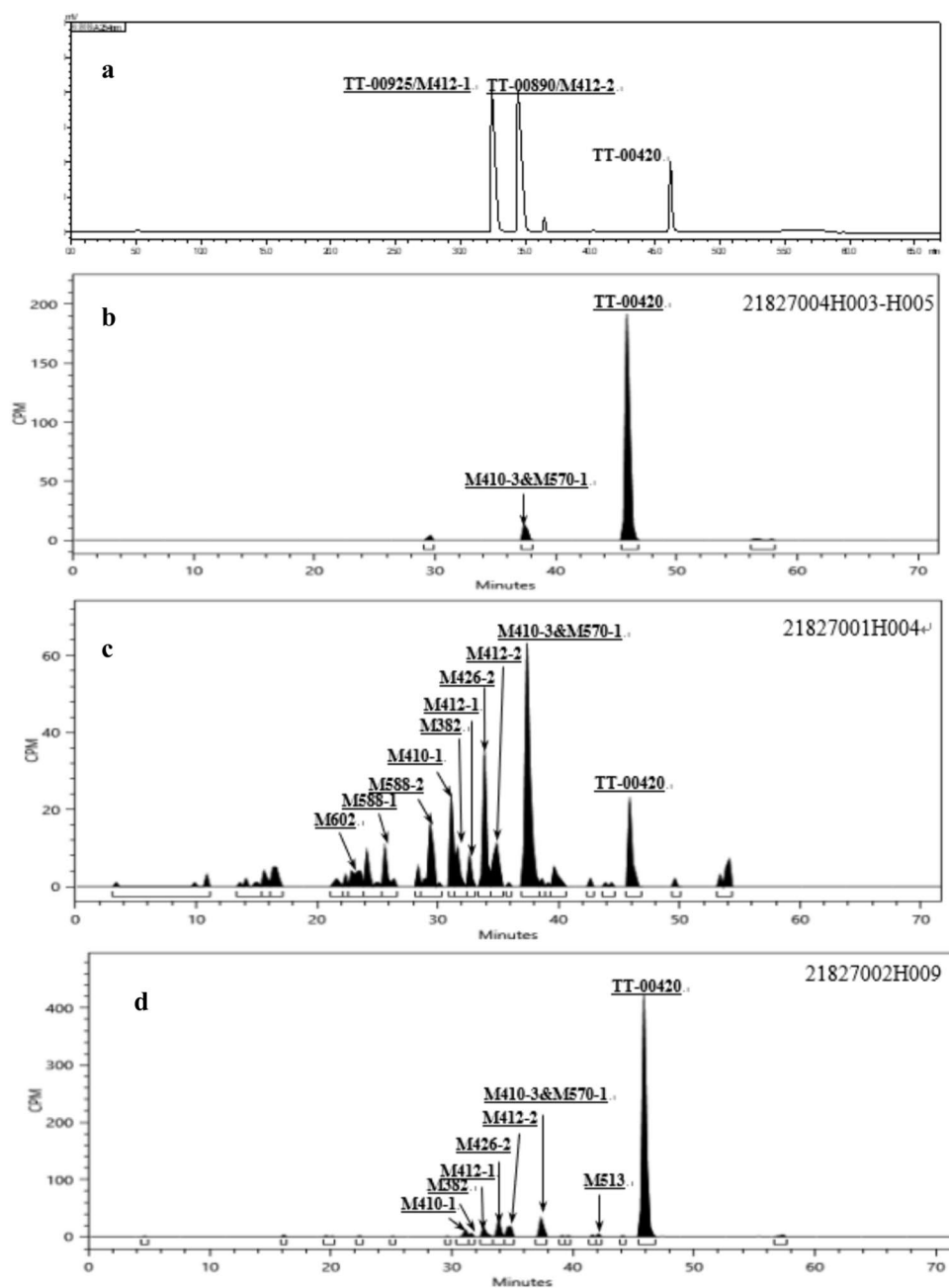
<sup>c</sup>Peak area of a single radioactive peak did not exceed 1.50% AUC, or 5.00% dose

<sup>d</sup>Proportion of identified radioactive peaks in current matrix

fragments of the parent compound characterized by mass spectrometry and/or by comparison with authentic reference standards. The measured mass and theoretical mass

values of the metabolites are described in Supplementary materials section 2.

**Fig. 4** Ultraviolet (UV) chromatogram of mixed standards (**a**: mixed standards (STDs) UV and representative HPLC-radiochromatogram of the pooled human plasma (**b**:  $M_{0-120\text{ h}}$ ), urine (**c**:  $M_{0-72\text{ h}}$ ), and feces (**d**:  $M_{0-192\text{ h}}$ )



### 3.4.1 Plasma

A total of 5 radioactivity peaks were detected in AUC-pooled plasma, and the unchanged tinengotinib accounted for 88.23% of TRA. Metabolites M410-3 and M570-1 represented 4.75% and 2.54% of TRA, respectively, whereas M412-1 and M412-2 were identified as trace metabolites and were both 0.06%. In addition, a few minor metabolites peaks of radioactivity, accounting for less than

1.57% of TRA, were not identified due to extremely low concentrations.

### 3.4.2 Urine

In the 0–72 h pooled urine samples, a total of 11 radioactivity peaks were detected, but the unchanged tinengotinib was a negligible (only 0.28% of the dose), with glucuronide conjugation of tinengotinib (M570-1, 1.82%), glucuronidation



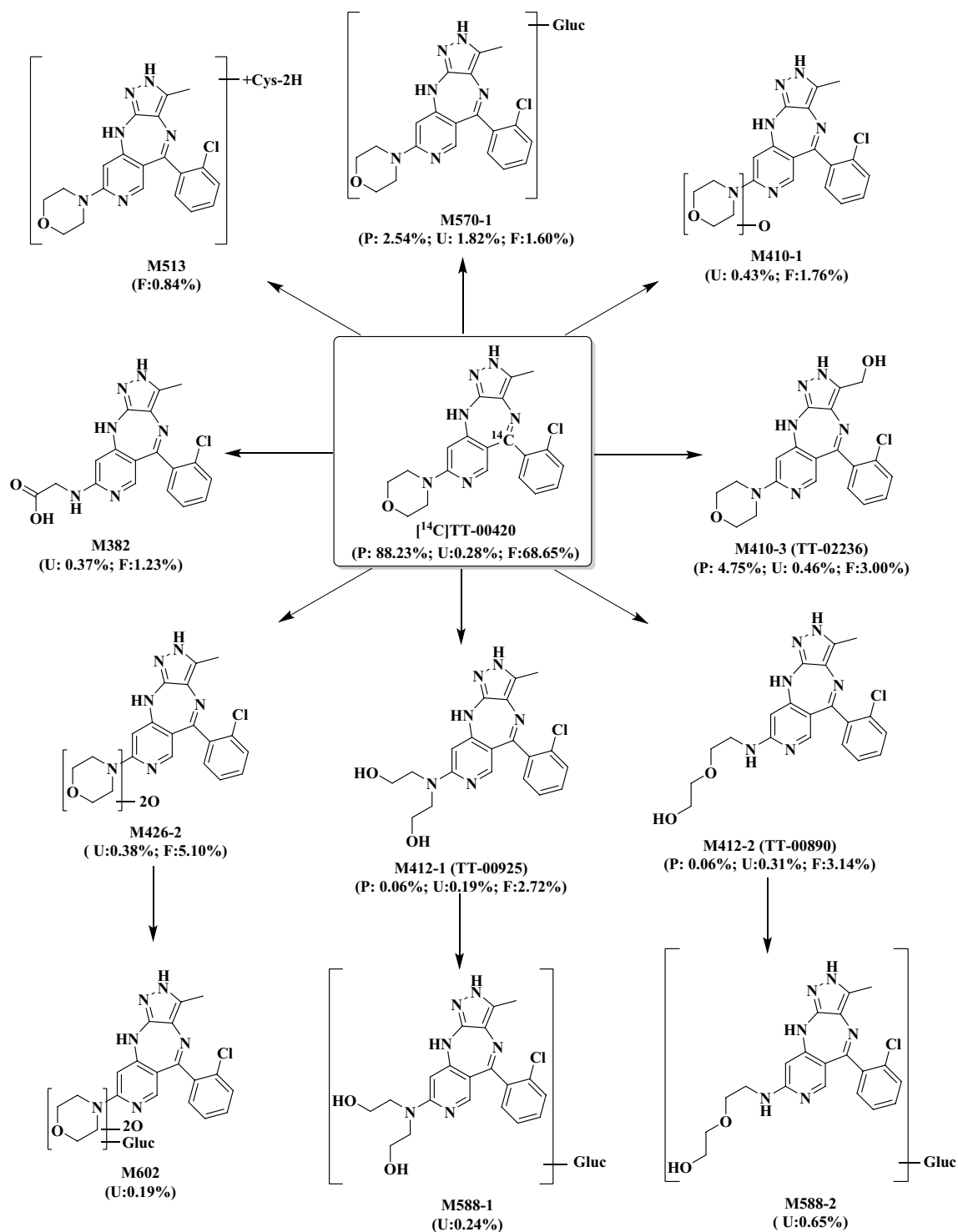


**Fig. 5** Proposed metabolic pathways of tinengotinib in human. Note: P, plasma (%AUC); U, urine (%Dose); F, feces (%Dose)

of oxidative tinengotinib (M588-2, 0.65% of the dose), and mono-oxidation (M410-3, 0.46%, and M410-1, 0.43%) representing the primary drug-related components in urine. The remaining metabolites did not exceed 0.40% of the dose.

### 3.4.3 Feces

In the 0–192 h pooled feces samples, a total of 9 radioactivity peaks were detected. The unchanged drug was the most abundant radioactive component in feces, accounting

for 68.65% of the dose, followed by di-oxidation (M426-2, 5.10%), oxidative cleavage of morpholine ring (M412-1, 2.74%, and M412-2, 3.14%), and mono-oxidation (M410-3, 3.14%). Other metabolites identified in feces accounted for less than 1.76% of the dose.

### 3.5 Phenotyping Assay

The negative control exhibited [ $^{14}\text{C}$ ]tinengotinib was stable after 120 min incubation without human recombinant P450 enzymes, non-P450 enzymes, HLM, or HL-S9. In addition to the parent tinengotinib, M410-1, M412-2, and M410-3 were detected after incubation with HLM or HL-S9, suggesting FMO3 or CYP450 enzymes may mediate the metabolism of tinengotinib. Tinengotinib was incubated with recombinant human non-CYP isozymes (FMO3, AO, and XO) and barely changed. After incubations with human rCYP3A4, rCYP2D6, and rCYP2C8, M410-1, M412-2, and M410-3 were detected in the rCYP3A4 incubation, accounting for 1.84%, 2.03%, and 0.02% of TRA, respectively, while rCYP2D6 and rCYP2C8 were not detected. These results suggest tinengotinib may be metabolized by CYP3A4 rather than CYP2D6 and CYP2C8.

## 4 Discussion and Conclusions

The design of this study is consistent with the most current practices for conducting human radiolabeled mass balance studies [10]. The radioactivity recoveries were completed with values ranging from 88.65 to 99.28% for sample preparation, and from 99.20 to 101.12% for HPLC column, respectively. The results showed that [ $^{14}\text{C}$ ]tinengotinib in plasma, urine, and fecal samples was stable during extraction procedures and HPLC analysis. The results also demonstrated that tinengotinib was not bound irreversibly to phospholipids, proteins, etc.

### 4.1 Pharmacokinetics and Mass Balance

The TRA and parent in plasma resulted in exposure values of 84.9 ng Eq/mL and 63.3 ng/mL on  $C_{\max}$ , and 2480 h-ng Eq/mL and 1640 h-ng/mL on  $\text{AUC}_{0-\infty}$ , respectively, which represents approximately 25.4% and 33.9% variance. The parent accounted for approximately 66.1% of the total plasma radioactivity  $\text{AUC}_{0-\infty}$ . Tinengotinib is rapidly absorbed with a median  $T_{\max}$  of 2 h, a low apparent clearance (6.2 L/h), a moderate apparent terminal volume of distribution (210 L), and a long terminal half-life (23.7 h). As shown in Fig. 2, the mean plasma concentrations for the TRA and parent versus time curves were comparable, with less gaps over 120 h after administration. These results suggested that most of the circulating radioactivity was comprised of unchanged

tinengotinib. However, the  $t_{1/2}$  value of TRA in plasma was longer than that of the parent tinengotinib, indicating the small amounts of metabolites with slower elimination rate limited clearance. The absorption fraction ( $F_a$ ) was estimated to be at least 30.92% of the dose, on the basis of the amount of radioactivity recovered in urine (7.11%) and the amount of metabolite excreted in feces (23.81%).  $F_a$  could be higher than 30.92% of the dose, since part of the unchanged tinengotinib in feces could have come from glucuronide conjugation metabolite (M570-1) that was reverted to the parent form through glucosidase in the gastrointestinal (GI) tract or from the absorbed parent drug that returned to the GI tract via biliary excretion. The mean whole blood-to-plasma total radioactivity ratios per time point were less than 1 and ranged from 0.794 to 0.827 up to 24 h post-dose, indicating no special affinity of tinengotinib or its metabolites to blood cells.

After oral administration of [ $^{14}\text{C}$ ]tinengotinib, the mean total recovery of radioactivity in excreta over 288 h post-dose exceed 99% of the dose, with 92.46% excreted into in feces and 7.11% in urine, which indicates a complete mass balance with small inter-individual variability (< 1%). According to previous research [8], there were no significant differences in excretion pathways between human and dog or rat in mass balance studies. The cumulative excretion of total radioactivity recovery occurred mainly in the first 120 h post-dose, with 92.52% of the dose in urine and feces. This study found that renal excretion only accounted for a minor part (< 10%) and played an insignificant role in the disposition of tinengotinib. Overall, the excretion of tinengotinib was predominantly through feces.

### 4.2 Metabolism

In the plasma samples, metabolites accounted for approximately 95.64% of the total radioactivity. The predominant drug-related component in human plasma was the unchanged drug tinengotinib, which represent 88.23% of TRA. Oxidation was identified as the primary route of metabolism, with the primary oxidation circulating metabolite, M410-3, accounting for 4.75% of the plasma total radioactivity and 5.38% of the parent drug in terms of  $\text{AUC}_{0-120\text{h}}$ . Each metabolite identified in plasma represented less than 2.54% of the total drug-related exposure for all subjects. Meanwhile, M410-3 accounted for 4.03%, 6.32%, 3.30%, and 3.70% of the total radioactivity in plasma at the 0.5 h, 2 h, 8 h, and 24 h time points. These results suggest that the time of sample collection did not influence changes in the proportion of the metabolite. Overall, the contribution of circulating human metabolites to activity did not exceed 25% of that of the parent drug. Therefore, the results of the present study suggested that tinengotinib was minimally metabolized, producing only four metabolites identified in

circulation, and none of these metabolites exceeded 5% of overall parent exposure. In addition, there were no unique human metabolites found.

The radioactivity identified in urine and feces accounted for 93.36% of the dose or 93.76% of the recovered radioactivity. In feces, with 92.46% of the dose excreted, unchanged tinengotinib was the prominent component accounting for 68.65% of the dose, followed by M426-2 (5.10%), and then other minor single metabolites (did not exceed 3.10% of the dose). In urine, with only 7.11% of the dose excreted (0.28% as unchanged), the phase II metabolites were the major drug-related components (2.90% of the dose). The drug-related component was excreted mostly in the feces in the form of the parents. Previous studies show that tinengotinib is not a substrate for major transporters [8]. Therefore, impaired renal function is not likely to affect the PK behavior of tinengotinib or its metabolites in patients because there is negligible renal excretion. These results provide justification for why we do not need to launch a dedicated renal impairment study based on the guidance from the FDA [11].

On the basis of the metabolite identification results obtained in this study, tinengotinib constituted the majority (88.23%) of the drug-related exposure in human plasma. Three minor metabolites were also identified, with each representing < 5% of the drug-related exposure. The biotransformation of tinengotinib in humans involves three main metabolic pathways: (1) oxidation or di-oxidation, (2) oxidative cleavage of morpholine ring, and (3) cystein or glucuronide conjugation. These findings were consistent with the metabolic pathways identified in preclinical studies.

### 4.3 Drug–Drug Interaction

In the previous non-radioactive predictive test studies [8], chemical inhibition method showed that the percentage metabolic rates of CYP3A4, 2D6, and 2C8 were 37.5%, 24.5%, and 20.0%, respectively, while the recombinant enzyme method indicated that tinengotinib was mainly metabolized by CYP3A4. In the current study, the human recombinant CYP isozymes (3A4, 2C8, and 2D6) and non-CYP isozymes (FMO3, AO, XO) were incubated with [<sup>14</sup>C]tinengotinib to confirm whether the metabolites observed in plasma could be monitored. The results showed that relevant plasma metabolites were detected in human rCYP3A4, but no metabolites were detected in recombinant human rCYP2C8, 2D6, FMO3, AO, and XO. The most significant finding to emerge from the analysis was that tinengotinib has limited metabolism, mainly via CYP3A4.

However, there were no metabolic enzymes involved in metabolic pathways that contributed to more than 25% of drug elimination, and no circulating metabolites that accounted for more than 10% of the total drug-related exposure in plasma were observed. These results suggest

tinengotinib is metabolically stable. Taken together, it could be hypothesized that tinengotinib is unlikely to exhibit significant ethnic sensitivity based on its PK properties.

As shown, tinengotinib is metabolized by CYP3A4, but rarely metabolites, suggesting that CYP450 inhibitors or inducers may have less impact on tinengotinib exposure. As per the guideline [12–14], no further studies are needed to evaluate metabolite-mediated safety and DDI potential. Taken together, tinengotinib showed minimal potential for perpetrating transporter- and enzyme-mediated DDIs with co-administered drugs [8]. However, considering that CYP3A4 inhibitors or inducers are widely used in clinical practice, the concomitant use of tinengotinib with a strong CYP3A4 inhibitor (e.g., itraconazole) or inducer (e.g., rifampin) will be explored in clinical pharmacological trials in healthy volunteers to evaluate the DDI potential.

### 4.4 Conclusions

In conclusion, the human mass balance study in this paper provides guidance for the clinical pharmacology development program, including DDI potential and special populations (i.e., renal or hepatic impairment) investigations, and helped validate the animal species used in toxicology studies.

**Supplementary Information** The online version contains supplementary material available at <https://doi.org/10.1007/s40268-024-00486-2>.

**Acknowledgements** The authors would like to express their sincere gratitude to the study participants. The authors sincerely thank the healthy subjects and all the staff who participated in the clinical trials.

### Declarations

**Funding** This work was funded by TransThera Sciences (Nanjing), Inc.

**Conflicts of Interest** Jean Fan is an employee of Trans Thera Sciences (US), Inc., which is a wholly owned subsidiary of TransThera Sciences (Nanjing), Inc. Shumao Ni, Yingying Yu, Yujia Zhu, Xiaofen Sun, Lin Li, Caixia Sun, Hui Wang, Peng Peng, and Frank Wu are all employees of TransThera Sciences (Nanjing), Inc. Shumao Ni, Sheng Ma, Yingying Yu, Zhenwen Yu, Yujia Zhu, Xiaofen Sun, Lin Li, Caixia Sun, Hui Wang, Peng Peng, Zheming Gu, Hua Zhang, Frank Wu, Liyan Miao, and Jean Fan have no conflicts of interest that are directly relevant to the content of this article.

**Data Availability** All data used and/or analyzed during this study are available from the corresponding author on reasonable request.

**Ethics Approval** The study was conducted in compliance with the Helsinki Declaration and the International Council for Harmonization Good Clinical Practice guidelines and approved by the Hospital Ethics (Ethics approval number: 2021230, 12 October 2021).

**Consent to Participate** All subjects provided written informed consent prior to study initiation.

**Consent for Publication** Not applicable.

**Code Availability** Not applicable.

**Authors' Contributions** Shumao Ni and Sheng Ma contributed equally to this work. S.M.N. and J.F. were responsible for data analysis, interpretation of the data, drafting the manuscript, and final approval of the version to be published and were accountable for all aspects of the work in ensuring that questions or comments raised by the reviewers have been addressed and incorporated, and questions related to the accuracy or integrity are appropriately investigated and resolved. S.M.N., S.M., Y.Y.Y., Y.J.Z., C.X.S., P.P., H.Z., F.W., and L.Y.M. participated in study design. S.M., H.Z., and L.Y.M. participated in clinical trials for data acquisition. Z.W.Y. and Z.M.G. participated in data analysis. X.F.S. participated in the preparation of capsules. L.L. synthesized the reference substances. S.M.N., Y.Y.Y., and H.W. participated in project administration. P.P. and F.W. provided financial support. All authors reviewed the manuscript.

**Open Access** This article is licensed under a Creative Commons Attribution-NonCommercial 4.0 International License, which permits any non-commercial use, sharing, adaptation, distribution and reproduction in any medium or format, as long as you give appropriate credit to the original author(s) and the source, provide a link to the Creative Commons licence, and indicate if changes were made. The images or other third party material in this article are included in the article's Creative Commons licence, unless indicated otherwise in a credit line to the material. If material is not included in the article's Creative Commons licence and your intended use is not permitted by statutory regulation or exceeds the permitted use, you will need to obtain permission directly from the copyright holder. To view a copy of this licence, visit <http://creativecommons.org/licenses/by-nc/4.0/>.

## References

- Peng P, Qiang XY, Li GY, Li L, Ni SM, Yu Q, et al. Tinengotinib (TT-00420), a novel spectrum-selective small molecule kinase inhibitor, is highly active against triple negative breast cancer. *Mol Cancer Ther.* 2022;22(2):205–14. <https://doi.org/10.1158/1535-7163.MCT-22-0012>.
- Piha-Paul SA, Ileana-Dumbrava E, Janku F, Karp DD, Meric-Bernstam F, Rodon J, et al. Phase I study of TT-00420, a multiple kinase inhibitor, in patients with triple negative breast cancers and other advanced solid tumors. *Cancer Res.* 2020;80:3011. <https://doi.org/10.1158/1538-7445.AM2020-3011>.
- Piha-Paul SA, Xu B, Janku F, Dumbrava EE, Fu S, Karp DD, et al. Phase I study of TT-00420, a multiple kinase inhibitor, as a single agent in advanced solid tumors. *J Clin Oncol.* 2021;39:3090. [https://doi.org/10.1200/JCO.2021.39.15\\_suppl.3090](https://doi.org/10.1200/JCO.2021.39.15_suppl.3090).
- Al-Zahir MZ, AlAmeel T. Extrahepatic cholangiocarcinoma with prolonged survival: a case report. *J Med Case Rep.* 2017;11:357. <https://doi.org/10.1186/s13256-017-1519-5>.
- Yang X, Wang YL, Zhao JK, Rong HH, Chen YJ, Xiong MT, et al. Coordinated regulation of BACH1 and mitochondrial metabolism through tumortargeted self-assembled nanoparticles for effective triple negative breast cancer combination therapy. *Acta Pharma Sin B.* 2022;12:3934–51. <https://doi.org/10.1016/j.apsb.2022.06.009>.
- Henríquez I, Roach M III, Morgan TM, Alberto Bossi A, Junior A, Gómez JA, Abuchaibe O, et al. Current and emerging therapies for metastatic castration-resistant prostate cancer (mCRPC). *Biomedicines.* 2021;9:1247. <https://doi.org/10.3390/biomedicines9091247>.
- Piha-Paul SA, Xu BH, Kanwal PSR, Funda MB, Filip J, et al. First-in-human, phase I study of TT-00420, a multiple kinase inhibitor, as a single agent in advanced solid tumors. *Am Soc Clin Oncol.* 2022. [https://doi.org/10.1200/JCO.2022.40.16\\_suppl.3013](https://doi.org/10.1200/JCO.2022.40.16_suppl.3013).
- Ni SM, Li L, Sun XF, Wang YX, Yu Q, Wang WW, et al. *In vitro* and *in vivo* pharmacokinetics, disposition, and drug-drug interaction potential of tinengotinib (TT-00420), a promising investigational drug for treatment of cholangiocarcinoma and other solid tumors. *Eur J Pharm Sci.* 2024. <https://doi.org/10.1016/j.ejps.2023.106658>.
- Hop CE, Wang Z, Chen Q, Kwei G. Plasma-pooling methods to increase throughput for *in vivo* pharmacokinetic screening. *Journal of Pharm Sci.* 1998;87:901–3. <https://doi.org/10.1021/js970486q>.
- Ramamoorthy A, Bende G, Chow ECY, Dimova H, Hartman N, Jean D, et al. Human radiolabeled mass balance studies supporting the FDA approval of new drugs. *Clin Transl Sci.* 2022;15:2567–75. <https://doi.org/10.1111/cts.13403>.
- Food and Drug Administration. Pharmacokinetics in patients with impaired renal function — study design, data analysis, and impact on dosing guidance for industry. March 2024, <https://www.fda.gov/media/78573/download>.
- Food and Drug Administration. Safety testing of drug metabolites guidance for industry. Mar 2020, <https://www.fda.gov/media/72279/download>.
- European Medicines Agency. Drug interaction guideline on the investigation of drug interactions. CPMP/EWP/560/95/Rev. 1 Corr. 2\*\*. June 2012, [https://www.ema.europa.eu/en/documents/scientific-guideline/guideline-investigation-drug-interactions-revision-1\\_en.pdf](https://www.ema.europa.eu/en/documents/scientific-guideline/guideline-investigation-drug-interactions-revision-1_en.pdf).
- The International Council for Harmonisation of Technical Requirements for Pharmaceuticals for Human Use (ICH), 2022. Drug Interaction Studies M12 (Draft version). [https://database.ich.org/sites/default/files/M12\\_Step1\\_draft\\_Guideline\\_2022\\_0524.pdf](https://database.ich.org/sites/default/files/M12_Step1_draft_Guideline_2022_0524.pdf).